Preliminary Development and Evaluation of Lightning Jump Algorithms for the Real-Time Detection of Severe Weather

Christopher J. Schultz *

Department of Atmospheric Science, The University of Alabama in Huntsville, Huntsville, Alabama

Walter A. Petersen

NASA Marshall Space Flight Center, Huntsville, Alabama

Lawrence D. Carey

Earth Systems Science Center, University of Alabama Huntsville, Huntsville, Alabama

* *Corresponding author address:* Christopher J. Schultz, Department of Atmospheric Science, The National Space Science and Technology Center, University of Alabama in Huntsville, 320 Sparkman Drive, Huntsville, AL 35805.

E-mail: schultz@nsstc.uah.edu

ABSTRACT

Previous studies have demonstrated that rapid increases in total lightning activity (intracloud + cloud-to-ground) are often observed tens of minutes in advance of the occurrence of severe weather at the ground. These rapid increases in lightning activity have been termed "lightning jumps." Herein, we document a positive correlation between lightning jumps and the manifestation of severe weather in thunderstorms occurring across the Tennessee Valley and Washington D.C. A total of 107 thunderstorms were examined in this study, with 69 of the 107 thunderstorms falling into the category of non-severe, and 38 into the category of severe. From the dataset of 69 isolated non-severe thunderstorms, an average peak 1 minute flash rate of 10 flashes min^{-1} was determined. A variety of severe thunderstorm types were examined for this study including an MCS, MCV, tornadic outer rainbands of tropical remnants, supercells, and pulse severe thunderstorms. Of the 107 thunderstorms, 85 thunderstorms (47 non-severe, 38 severe) from the Tennessee Valley and Washington D.C tested 6 lightning jump algorithm configurations (Gatlin, Gatlin 45, 2σ, 3σ, Threshold 10, and Threshold 8). Performance metrics for each algorithm were then calculated, yielding encouraging results from the limited sample of 85 thunderstorms. The 2σ lightning jump algorithm had a high probability of detection (POD; 87%), a modest false alarm rate (FAR; 33%), and a solid Heidke Skill Score (HSS; 0.75). A second and more simplistic lightning jump algorithm named the Threshold 8 lightning jump algorithm also shows promise, with a POD of 81% and a FAR of 41%. Average lead times to severe weather occurrence for these two algorithms were 23 minutes and 20 minutes, respectively. The overall goal of this study is to advance the development of an operationally-applicable jump algorithm that can be used with either total lightning observations made from the ground, or in the near future

from space using the GOES-R Geostationary Lightning Mapper.

1. Introduction

Numerous studies have demonstrated the potential utility of total lightning data for use in decision support during severe weather situations (Goodman et al. 1988, MacGorman et al. 1989, Williams 1989a, Williams et al. 1999, Buechler et al. 2000, Goodman et al. 2005, Bridenstine et al. 2005, Wiens et al. 2005, Steiger et al. 2005, Gatlin 2006, Steiger et al. 2007). These previous studies have found positive correlations between rapid increases in total lightning, also termed *lightning jumps* (Williams et al. 1999), and manifestations of severe weather at the surface. Of course not all severe weather is preceded by a lightning jump, nor do all storms that produce these rapid increases in lightning contain severe weather. Yet, despite occasional ambiguities, numerous concrete examples of increases in lightning several minutes prior to severe weather have been observed in thunderstorms across Alabama, Tennessee, Florida, Texas, Oklahoma and Colorado. The observations are a manifestation of the physical links between cloud dynamics, microphysics. and thunderstorm electrification.

Thunderstorm electrification is currently thought to be dominated primarily by the non-inductive charging process (NIC; Takahashi 1978, Saunders et al. 1991). More specifically, NIC involves charge transfer between ice crystals and graupel or hail particles in the presence of supercooled liquid water. The combination of a thunderstorm updraft and the Earth's gravitational force then provide the necessary cloud scale separation of charge within the cloud, thus forming an electric field. As charge continually builds over time, the electric field

reaches a breakdown magnitude, and lightning occurs. Collectively, numerous observational studies have presented evidence to support the dominance of NIC processes in thunderstorms.

Workman and Reynolds (1949) were some of the first to show that the amount of lightning produced by a thunderstorm is closely tied to updraft evolution and appearance of an ice phase. Vonnegut (1963), Williams (1985), and Boccippio (2002) demonstrated that a nonlinear relationship exists between storm depth and the amount of lightning a storm produces. Thus, thunderstorms having stronger updrafts (e.g., severe thunderstorms) have the potential to produce more lightning. Carey and Rutledge (1996), Carey and Rutledge (2000), Petersen et al. (2005) and others provide strong evidence linking precipitation ice mass to lightning occurrence and amount, while Deierling (2006) linked the ice mass and updraft to lightning occurrence by demonstrating correlation between the vertical flux of ice and the total flash rate. Given the strong correlation between the dynamics and microphysical evolution of the thunderstorms and lightning production, it seems reasonable to assume that lightning activity would provide some indication of storm severity.

In the mid to late 1980's Goodman et al. (1988) and Williams et al. (1989a) correlated total lightning rates to the onset of wet microbursts in Northern Alabama. MacGorman and Rust (1989) also observed increases in total lightning in a tornadic thunderstorm near Binger, Oklahoma in 1981. In the past decade, many studies continued to find similar findings. Williams et al. (1999) found increases in the total flash rate prior to severe weather in several thunderstorms in Florida. Goodman et al. (2005) demonstrated similar results for tornadic thunderstorms in South Central Tennessee, as well as for a damaging microburst case near Huntsville, AL in August of 2002. Wiens et al. (2005) demonstrated that these

increases in lightning also occur across the High Plains, as observed during the STEPS field project in 2000 (Lang et al. 2004). Wiens as well as Tessendorf et al. (2005, 2007) compared lightning rates to updrafts and graupel/hail volume using dual Doppler analysis. Other noteworthy studies can be found from the Dallas total lightning network (e.g., Steiger et al. 2005, Wilson et al. 2006, Steiger et al. 2007). Gatlin (2006) described numerous lightning jumps that occurred prior to the onset of severe thunderstorms in the Tennessee Valley, and his work utilized the time rate of change of the total flash rate as a predictor for defining a jump in the total amount of lightning.

Gatlin (2006) provided the basic framework for an operational algorithm that could be used by a warning forecaster to assess a storm's severity through the incorporation of total lightning data. In Gatlin's framework, the time rate of change of the total flash rate, relative to a running background mean, provided the means to nowcast the occurrence of severe weather at the surface with a lead time as large as 25 minutes (Goodman et al. 2005). However, Gatlin's analysis and framework were limited by 1) the lack of a broad spectrum of case study types, 2) and no assessment of total lightning behavior in ordinary non-severe thunderstorms, and how non-severe thunderstorms may affect the performance of an operational algorithm. The first limitation has significance because not all severe weather-producing storms are isolated. The second limitation is important because all thunderstorms will, by definition, exhibit at least one jump in lighting activity during their lifetime (i.e., prior to first lightning in the cumulus stage or later impulsive changes associated with pulsing growth in the latter mature and dissipating stages; Byers and Braham (1949)). These pulses in activity can conceivably lead to warning false alarms if lightning jump criteria are used for thunderstorms that are clearly below severe limits, thus creating a lack of confidence in the

operational product.

The purpose of this study is to extend the Gatlin (2006) framework by investigating the link between total lightning and the occurrence of severe weather over a *wide* range of thunderstorm types. Based on the results, the aim is also to provide a new lightning jump methodology for improving lead times and forecaster confidence during the severe thunderstorm warning process, allowing for more timely and accurate warnings. Ultimately we plan to build on the method during continued development of an operational algorithm for use in the Geostationary Operational Environmental Satellite Series R (GOES-R) Lightning Mapper data stream (Goodman et al. 2006).

2. Data and Methodology

Development of an operational algorithm for thunderstorm warnings using lightning data requires the the following steps. First, severe and non-severe thunderstorms must be identified and partitioned for different regions. Secondly, the lighting flash behavior for non-severe thunderstorms must be quantified to understand trends that occur in "everyday" non-severe thunderstorms. This step provides a "behavioral background" from which severe thunderstorms should stand out. Third, algorithms must be formulated and tested for the identified thunderstorm types. The algorithm providing the best "performance" can be further refined (if needed) to create an operational algorithm for real-time use.

a. Case Selection

Thunderstorm cases were primarily chosen from 2 regions of the U.S. One region is located in the Tennessee Valley, which is comprised of Northern Alabama and South Central Tennessee. The second region is the Washington D.C. Metro area. Both locations are covered by Doppler radar, and very high frequency (VHF) total lightning mapping array systems. The period of study was from 2002 to 2008 for severe thunderstorms, while non-severe thunderstorms were limited only to the warm season during this period, defined as May through September. Non-severe thunderstorms were defined as those thunderstorms having 1) an isolated 35 dBZ reflectivity contour evident at 2 km for at least 30 minutes, 2) no report of severe weather, 3) isolation from other convection. Severe thunderstorm cases were chosen based on present National Weather Service (NWS) criteria, which require the presence of 1) hail $\geq$ 1.9 cm, 2) wind $\geq$ 26 m s^{-1}, and/or 3) the occurrence of a tornado. In order to study *all* severe thunderstorms and isolate the "core" feature, a 35 dBZ contour is tracked at the -15°C isotherm. This level is well within the temperature range needed for thunderstorm charging. The use of a 35 dBZ threshold provides a means to isolate the most vigorous updrafts and thunderstorm precipitation cores.

b. Severe Weather Reports

The locations, magnitudes and timing of observed severe weather events were obtained from the National Oceanic and Atmospheric Administration's (NOAA) National Climatic Data Center's (NCDC) *Storm Data.* Unfortunately, there are several documented cases of

errors in reporting times and magnitudes (e.g., Witt et al. 1998b, Williams et al. 1999, Weiss et al. 2002, Trapp et al. 2005); however, this data set is the most accurate in trying to determine what exactly occurred as a severe storm passed over a given location. Witt et al. (1998b) observed that 38% of tornado report times were not within 5 minutes of the actual occurence in 26 tornado days studied. According to Williams et al. (1999), only 10% of all storm data are likely to be accurate within 1 minute of occurrence. Furthermore, another 15% fall within the 2 to 5 minute range. Finally an additional 50% of reports fall into the 6 to 10 minute range. These inaccuracies in report time contribute to ambiguities in the determination of lead times between lighting jumps and severe weather. Williams et al. (1999) also noted that the more severe an event is, the more accurate the report time becomes. Weiss et al. (2002) and Trapp et al. (2005) show discontinuities in the number of wind reports and magnitudes between NWS offices. They also note that many of the wind reports over the past 10 years are estimated, and not measured winds, which then leads to discrete maxima in reports at wind speeds of 50, 55, 60, 65, and 70 kts. Despite these errors, the dataset provided by NCDC is still the most accessible and accurate in determining what exactly occurs during severe storm events. Additional care was taken to manually go through each report and assign viable reports to specific severe storms.

c. Total and Cloud-to-Ground Lightning Information

Total lightning flashes were observed using 2 very high frequency (VHF) Lightning Mapping Arrays (LMA; Rison et al. 1999, Krehbiel et al. 2000, Wiens et al. 2005, Goodman

et al. 2005) located in Northern Alabama (Koshak et al. 2004) and in Washington D.C. (Krehbiel 2008). The North Alabama LMA consists of 10 receiving stations with a central processing site located at the National Space Science and Technology Center (NSSTC) in Huntsville, AL. The Washington D.C. Lightning Mapping Array (DCLMA) is similar in nature, but consists of 8 stations located throughout Maryland, Northeastern Virginia and Washington D.C, and the DCLMA data are collected and reprocessed at the NSSTC. The North Alabama LMA operates in the 76-82 MHz range (Television Channel 5), while the DCLMA operates in the upper VHF (Channel 10) range. Each station in the LMA measures VHF radio frequency pulses in 80 μs intervals and calculates a position for each VHF lightning source using GPS and time of arrival (TOA) methods using at least 6 stations in the array. Lightning sources are then combined to map a lightning flash in three dimensions to highlight the lightning channel (Proctor 1971). Part of the data is then sent in real-time to the NSSTC, where it is reprocessed and distributed to select NWS forecast offices for use in severe storm decision making. The full dataset is collected from each station and then post-processed to create a complete dataset for research purposes.

To obtain the full three-dimensional view of a flash, as well as eliminate noise points within the LMA dataset, the VHF source points are combined using a clustering algorithm that combines data points in both space and time. For the North Alabama LMA, VHF sources that occur within 0.3 seconds and 0.5 radians of azimuth are clustered together as a first step in identifying a given "flash". Next a network range requirement is used, and is based on the range of the potential flash from the center of the LMA. This clustering algorithm does not place an upper threshold on the temporal length of a flash; however, comparisons with other studies (e.g., Thomas et al. 2004) show good agreement in the num-

ber of flashes. The DCLMA uses a different clustering algorithm which is found in the LMA display package named XLMA. However, XLMA combines VHF sources with similar space and time criteria (Thomas et al. 2004).

Herein we require each flash to be comprised of a minimum of 10 VHF sources for increased accuracy in flash length determination. Wiens et al. (2005) demonstrated that a minimum source threshold in LMA data will not affect the determination of the *trend* in total lightning, thus the 10 source minimum will not have an adverse effect in calculating the time rate of change in the flash rate. Thresholding at 10 VHF sources also eliminates noise points that the LMA might misclassify as sources and subsequently be used for flash determination. Additionally, 2 range thresholds are set to see how distance from the LMA center affects lightning measurements and each lightning jump algorithms. The first range threshold is set at 150 km, and second range threshold is set at 100 km. These two range thresholds fall within the 160 km range threshold determined in Koshak et al. 2004, where spatial errors in source location approach a maximum of 50 m at that range.

Ground flashes are determined from the National Lightning Detection Network (NLDN) which is comprised of 113 sensors across the United States with a flash detection efficiency of 90-93% (Cummins et al. 2006). The network occasionally misclassifies small positive IC flashes as postive CG flashes; therefore, a +15 kA peak current threshold is applied to accurately estimate positive CG flash counts (Biagi et al. 2007).

d. Radar Data and Thunderstorm Tracking

Radar data are extensively used in this study for cell tracking, determining storm intensity, and comparing with lightning data. Next Generation Weather Radar (NEXRAD) data were retrieved from NOAA's NCDC in archived Level II format. These data were collected from five NWS Weather Surveillance Radar-1988 Doppler (WSR-88D; Crum and Alberty 1993) located at Hytop, AL (KHTX), Calera, AL (KBMX), Columbus Air Force Base, MS (KGWX), Old Hickory, TN (KOHX), and Sterling, VA (KLWX). The first four radars listed surround the North Alabama LMA, while the final radar listed is centered in the domain of the DCLMA. Radar data were transformed from its native Level II format using 2 different methods. Each method serves its own purpose for tracking as well as determining a storm's intensity.

The first method of transformation is used for cell tracking purposes. Level II reflectivity was transformed from polar coordinates (i.e., radar space) to a 2 km x 2 km x 1 km Cartesian grid using a 0.9° radius of influence in the REORDER software (Oye and Case 1995) developed by the National Center for Atmospheric Research (NCAR). The grid size is 300 km x 300 km x 19 km with the origin centered over each individual radar. Reflectivity grids are then fed into the Thunderstorm Identification, Tracking and Nowcasting algorithm (TITAN; Dixon and Wiener 1993) and each storm that meets the desired temperature and height criteria is tracked.

The second method for transforming the radar data is similar to the first; however, there are some notable differences. The radar data were taken from its native Level II format to network common data form (NETCDF) using the Warning Decision Support System-

Integrated Information (WDSS-II) (Lakshmanan et al. 2006, Lakshmanan et al. 2007). Latitude, longitude, height grids of reflectivity, azimuthal shear, and vertically integrated liquid (VIL) were then created using grid spacing of 1 km x 1 km x 1 km on a grid size of 300 km x 425 km x 19 km for each data product. In order to have a common areal domain for all radars and the LMA, grids were centered on the NSSTC for the North Alabama cases, and on the NWS forecast office in Sterling, VA for the Washington D.C. cases.

e. Jump Algorithm Approaches

Many methods can be used to predict storm severity based on total lightning trends in thunderstorms. In this study, 6 algorithm configurations are examined to determine which may be the best for a real-time operational lightning jump algorithm. Range dependence, warning length and minimum flash thresholds are explored to maximize the utility of each algorithm.

1) A Summary of the Gatlin Algorithm

Gatlin (2006) created a multi-step framework for an operational algorithm to be used to determine storm severity. First, Gatlin (2006) computes the average flash rate over a 2 minute period.

$$FR_{avg}(t_i)(flashes\ min^{-1}) = \frac{FR_{t1}(t_1) + FR_{t2}(t_2)}{2}. \quad (1)$$

$FR(t)_{t1}$ and $FR(t)_{t2}$ are the 1 minute total lighting counts from a thunderstorm, and FR_{avg} is the 1 minute averaged flash rate that is calculated every 2 minutes. Next, a weighted moving average is determined from the three previous 2 minute periods of data (lasting 6 minutes) using

$$\overline{f(t_3)}(flashes\ min^{-1}) = \frac{1}{3}(FR_{avg}(t_3) + \frac{2}{3}FR_{avg}(t_2) + \frac{1}{3}FR_{avg}(t_1)), \quad (2)$$

where $FR_{avg}(t_1)$, $FR_{avg}(t_2)$, and $FR_{avg}(t_3)$ are computed as in (1). Once another time period is calculated (e.g., $\overline{f(t)_4}$, then the trend in the total flash rate at t_4, DFRDT, can be calculated using

$$\frac{d}{dt}\overline{f(t_4)} = \frac{\overline{f(t_4)} - \overline{f(t_3)}}{t_4 - t_3} = DFRDT(flashes\ min^{-2}). \quad (3)$$

A standard deviation in DFRDT is then calculated using the most recent three DFRDT values. The current standard deviation value is averaged with the previous time step's standard deviation value to obtain a new lightning jump threshold value. A trend is considered a jump once the DFRDT value exceeds one standard deviation above the mean DFRDT value and ends when the DFRDT value falls below zero.

2) Threshold Algorithms

A simple technique explored in this study is termed the "threshold" method. The purpose of the threshold method is to delineate between a storm that is severe and one that is non-severe based on climatologically observed conditions. Some overlap between the 2 classifications of severity is expected; however, a simple method such as this one might provide useful information in real-time situations as the threshold algorithms are not computationally tasking.

In this technique 2 different thresholds are used for delineating between severe and non-severe thunderstorms. The first threshold used is based on the peak 1 minute total flash rate (e.g., Williams et al. 1999), and the second is based on the DFRDT value. The importance of the peak flash rate threshold is that it essentially activates the algorithm, while the value of the second threshold DFRDT then determines if the lightning activity is associated with a severe or non-severe thunderstorm. The peak 1 minute flash rate threshold is based on a survey of 69 non-severe thunderstorm cases observed in three different areas having total lightning networks. 47 of these storms occurred in North Alabama, while the remaining 22 occurred near Lightning Detection and Ranging (LDAR) networks around Houston and Dallas, TX (Motley 2006). From these cases we diagnose the mean to be 10 flashes min^{-1} (Figure 1).

The maximum DFRDT threshold value for each of the non-severe thunderstorm was also calculated using the difference in the 1 minute average flash rate (Equation 3). DFRDT thresholds were determined from the sample of non-severe thunderstorms presented in Figure 2. Thresholds were arbitrarily chosen at the 90^{th} and 93^{rd} percentile, which turned out

to be 8 flashes min^{-2} and 10 flashes min^{-2}, respectively. As stated above, some overlap is expected between the severe/non-severe partition, hence a 5-10% false alarm rate (FAR) for identification of a severe thunderstorm is already assumed. Currently, the FAR for severe thunderstorm and tornado warnings combined for the entire NWS is around 48% (Barnes et al. 2007); for tornadoes only, the FAR value is 76%. 2 DFRDT thresholds were tested to evaluate the variablility in probability of detection as a function of false alarm rate.

Relative to the 90-93% levels discussed above, an algorithm referred to as the Threshold 10 algorithm is defined, and activates the jump algorithm when the total flash rate equals or exceeds 10 flashes min^{-1} and DFRDT values exceed 10 flashes min^{-2} (for the 93% level). Likewise the Threshold 8 algorithm (90% level) uses the same type of flash rate criteria; however, the DFRDT barrier is set at 8 flashes min^{-2}.

3) The Sigma Algorithms

The "sigma" algorithm (σ = standard deviation) we develop are a variant of the Gatlin algorithm; however, they involve less smoothing of the data and higher jump thresholding to lower false alarm rates. 1 minute flash rates are calculated as in Equation 3, and similarly DFRDT values are computed from these 1 minute averaged totals. A standard deviation calculation is based on the most recent five periods of time (i.e., the previous ten minutes), not including the period of interest. Next we consider a 2σ variation from the running mean behavior to identify abnormal lightning behavior. The 2σ was chosen on a trial and error basis to reduce the number of false alarms while still maintaining a high probability of de-

tection. A 2σ deviation eliminates smaller jumps, while still allowing for the detection of significant increases in lightning behavior. Similarly, a 3σ lightning jump algorithm configuration was also developed for further testing.

Finally, a 10 min^{-1} flash rate threshold is employed to the 2σ and 3σ algorithms so that normal behavior associated with non-severe thunderstorms, and non-severe stages of severe thunderstorms are not misclassified as severe. This threshold is based on the mean flash rate determined for non-severe storms discussed in the previous section. For the sigma algorithms, a "jump" occurs once the value of DFRDT exceeds the 2σ or 3σ threshold, respectively. A jump ends once the DFRDT value is less than or equal to 0, unless 2 jumps are separated by 6 minutes or fewer. If 2 jumps are separated by 6 minutes or fewer (i.e., jump, no jump and jump in consecutive periods) this is counted as one jump.

4) Warning Length and Verification

Once a lightning jump occurs, a severe warning is placed on the thunderstorm for 45 minutes. This 45 minute period is the average warning length for severe thunderstorms provided by the NWS (T. Troutman, WCM WFO Huntsville, personal communication, 2008). Additionally, to facilitate comparison with the results of Gatlin (2006), a separate warning length of 30 minutes is also tested. The algorithm using the 30 minute warning time will be termed the "Gatlin algorithm", while the algorithm using the 45 minute warning length will be denoted as the "Gatlin 45" algorithm. Verification of a severe warning will occur if severe weather is observed within the warning time period. Events that are reported within

6 minutes of each other are counted as one event. Multiple events can occur within the warning period, and each is counted as a hit if a warning has been issued. If severe weather occurs while 2 warnings are in effect, the verification of the severe warning is counted toward the earliest issued warning that is still in effect. Severe weather events that occur without the presence of a lightning jump warning are misses. Lightning jump warnings that do not verify with a severe weather event are false alarms, including secondary lightning jumps that extend initial lightning jump warning times. To provide objective performance evaluation of the algorithms, contingency tables are created to analyze the success or failure of each algorithm. Probability of detection (POD), false alarm rate (FAR), and critical success index (CSI) are calculated for each algorithm over the entire dataset of thunderstorms (Wilks 1995, pp. 238-241). Heidke Skill Scores (HSS) are also calculated using a method by Doswell et al. (1990), which better accounts for rare events (like severe thunderstorms) to test the skill of each algorithm.

3. Results

a. Non-Severe Thunderstorms

Here non-severe thunderstorms are examined to set the basic framework for formulation of the lightning jump algorithm. Additionally, each algorithm is tested against the non-severe population to identify the number of false alarms a given non-severe sample might produce.

1) Characteristics

Determination of what is "normal" lightning behavior for a thunderstorm must first be considered prior to implementing an algorithm that identifies a storm as severe. For example, the overall sample of 69 non-severe thunderstorms from 2 different regimes yields an average peak flash rate for non-severe storms of 10.06 flashes min^{-1}. Furthermore, examining the DFRDT characteristics of the non-severe dataset reveals that the average peak DFRDT value of 4.74 flashes min^{-2}. Using the North Alabama cases, 90% of the non-severe thunderstorms fall below a threshold of 8 flashes min^{-2}, while 93% fall below a threshold of 10 flashes min^{-2}, and these 2 thresholds are the second part of the threshold technique. Importantly the average peak flash rate can be applied as a separate criterion for the 2σ, 3σ, and threshold algorithms for initialization. The DFRDT information is then used for creation of a second limit to determine whether or not a lightning jump occurs.

2) Testing of Algorithms on Non-severe Thunderstorms

The next step is to test the non-severe dataset against each of the algorithms to understand potential false alarm rates for misidentification of non-severe storms as severe. Table 1 shows the number of warnings that would be issued on the Northern Alabama dataset for non-severe thunderstorms using each lightning jump algorithm configuration. Leading the way in number of false alarms is the Gatlin methods with 92 false severe classifications. The

2σ algorithm produced significantly fewer false alarms for the non-severe dataset (16), and the 3σ came in with slightly fewer with 10 false alarms. The Threshold 8 and Threshold 10 algorithms round out the bottom with 7 and 6 false alarms, respectively.

b. Severe Thunderstorms

1) Case Examples

(i) 4 April 2007, MCS

A large linear MCS moved into the Tennessee Valley from the northwest during the late evening hours. This system developed in the Mid Mississippi Valley during the early afternoon on 3 April and plowed southeastward ahead of a strong cold front. Severe weather hail and high winds was already ongoing as the complex entered the domain of study. Using the 35 dBZ at -15°C isolation technique, several thunderstorm cells are identified within the convective line (Figure 3), which shows the utility of the isolation technique in complex convective situations.

One thunderstorm formed just to the north of the AL/TN border in Pulaski and Giles County, TN about 0245 UTC on April 4, 2007 (Figure 4, top left). This cell was located just ahead of the main MCS squall line that had produced severe hail and wind across Central Tennessee in Figure 3. Initially, total flash rates were only on the order of 10 min^{-1}, and the maximum height of the 35 dBZ contour was consistently found between 10 and 11 km (Figure 5). The MCS approached the area from the northwest and interacted with the devel-

oping storm about between 0300 and 0310 UTC. At 0305 UTC the NWS office in Huntsville issued a severe thunderstorm warning ahead of this section of the MCS. Coincident with the collision between the developing cell and convective line, the 35 dBZ height shot upward to 13 km around 0306 UTC. In response to the vertical growth and interaction with the bow echo, the total flash rate for the storm dramatically jumped from 23 flashes min^{-1} at 0257 UTC to 87 flashes min^{-1} at 0310 UTC (Figure 5). During this period all 6 algorithms triggered for this area. At the NWS WFO in Huntsville, the warning forecaster noted the flash rate on the AWIPS display was over 100 flashes min^{-1}.[1] Unfortunately with the current configuration of the lightning data at WFO Huntsville, it is is difficult for the warning forecaster to "eyeball sources and formulate jumps in their head, while still maintaining their warning duties" (C. Darden, SOO WFO Huntsville, personal communication, 2009). Around 0325 UTC a small EF0 tornado occurred near Taft, TN. This tornado then moved across the AL/TN state line and dissipated near the town of Hazel Green, AL at 0336 UTC. The report was not received by the NWS Huntsville until 0340 UTC, which demonstrates the problematic nature of severe weather event report times. Around 0330 UTC, a 65 dBZ maximum in reflectivity formed at an altitude of 5 km and dipped down to the surface. At 0334 UTC the NWS upgraded the severe thunderstorm warning for this part of the MCS to a tornado warning. At 0335 UTC several power poles were snapped off at the base near Maysville, AL, and at 0345 UTC 1.00 inch hail was reported in Flintville, TN. Again, it is emphasized that on average the lightning jump for this case occurred nearly 25 minutes in advance of the tornado touchdown, and over 30 minutes in advance of the destructive winds

[1]Real-time flashes at WFO Huntsville are actually real-time gridded source data. Sources are not pieced together to create flashes, but are named flashes for simplicity.

and hail across Northern Madison Co., AL and Southern Lincoln Co., TN. The lightning jump data in this case may have reinforced a warning decision if there were an operational lightning jump algorithm in place.

(ii) 25 September 2005, Tropical Cylone Tornado

On September 23, 2005, Hurricane Rita made landfall along the southeast coast of Texas, near the Texas/Louisiana border. Rita produced significant damage along this stretch of the Gulf Coast before moving inland. By September 25, 2005, the remnants moved into Central and Northern AL, and the system's outer bands produced several severe thunderstorms (Figure 6). One such thunderstorm spawned 2 tornadoes near Double Springs, AL. The severe thunderstorm that spawned the tornadoes initially developed outside of the maximum range set for this study (>150 km); however, by 1844 UTC the storm moved into the outer 150 km domain. Total flash rates for this storm were low at 1844 UTC (1-2 min^{-1}). At 1848 UTC the Gatlin algorithm sounded an alarm due to a slight increase in 1 minute averaged flash activity, demonstrating that the Gatlin algorithms are sensitive to small changes in flash rate. The lightning flash rate at this point increased from 1 flash min^{-1} to 2 flashes min^{-1}. From 1844 UTC to 1915 UTC, the vertical extent of the thunderstorm remained constant, with the 35 dBZ height extending up to 8 km, and the 50 dBZ height remaining around 5 km. However, the rotational velocity of the storm increased in the lowest levels of the thunderstorm. Azimuthal shear values noticeably increased for the next 50 minutes, with values ranging from $4x10^{-3}$ s^{-1} to $6.5x10^{-3}$ s^{-1}. This rotation was confined to the lowest

3 km of the storm.

Examining Figure 7, around 1920 UTC a 55 dBZ core developed aloft near a height of 4 km. By 1930 UTC the core extended up to 5 km and the 35 dBZ echo top height reached up to the 9 km height. Increases in height shown in the time-height plot (Figure 7) along with higher reflectivity values indicate that there were larger amounts of ice present aloft. In response to the vertical growth the total flash rate increased from 1 flash min^{-1} at 1923 UTC to 10 flashes min^{-1} by 1927 UTC. At this time the 10 flash threshold was met and 4 of the 6 algorithms warned on this potentially dangerous cell. Between 1943 UTC and 1948 UTC, the CG flash rate peaked at 3 CG flashes min^{-1}, all comprised of 100% negative polarity flashes. At 1954 and 1957 UTC 2 tornado reports are relayed to the NWS in Birmingham, and a tornado warning was issued.

For the Rita case, the lightning jump algorithm provides around 12 minutes of lead time for the Gatlin algorithms, while the 2σ and 3σ algorithms provide nearly 30 minutes of lead time. The 2σ and 3σ algorithms are less sensitive to thresholds but not independent of them. The Threshold algorithms do not provide any lead time because the flash rate does not meet all of the necessary requirements for a jump to be identified. The relative dearth of lightning in some tropical situations could pose potential problems for some lightning jump algorithms; however, the lightning data coupled with the radar data can add value to the warning decision process in tropical situations. For instance, the rotation within the storm was evident well in advance of the tornado (about 1 hr). In this instance, there was an increase in the vertical extent of the thunderstorm and the total flash rate, indicating potential stretching of the updraft and rotation within the thunderstorm. In this specific case, the lighting jump algorithm would have added valuable information to the NWS radar

operator for use in a real-time decision.

(iii) 4 July 2007, Washington D.C. Supercell

For the second straight year on July 4th, the Washington D.C. metro area experienced severe weather. Multiple isolated severe thunderstorms affected the area with wind and hail (Figure 8). The particular thunderstorm examined here developed along the Maryland-Virginia border at 1822 UTC and is located nearly due north of Washington D.C. in Figure 8. The storm pushed its way across Loudoun County, VA for the next hour, producing lightning rates of a few flashes per minute. Despite the relative lack of lightning, the thunderstorm developed a strong reflectivity >50 dBZ core, but the core was confined to the lowest 3 km of the atmosphere (temperatures warmer than -10°C). By 1900 UTC the core reflectivity increased to >60 dBZ, and the storm extended upwards to 6 km.

By 1934 UTC the 35 dBZ echo top height shot up to 9 km, and the thunderstorm was identified by the TITAN software. Even with the strong vertical growth of the thunderstorm, lightning flash rates increased only slightly to 6 to 10 per minute (Figure 9). The strong reflectivity core >50 dBZ descended by 1951 UTC, and at 2000 UTC 0.75 inch hail was reported at the surface. The Gatlin algorithms detected and triggered on a subtle increase in total lightning around 1950 UTC, where the flash rate increased from 3 flashes min^{-1} to 6 flashes min^{-1}; however, this again emphasizes the sensitive nature of the algorithm to minor increases in total flash rate. The remaining algorithms did not trigger because the flash rate remained below 10 flashes min^{-1}.

At 2008 UTC, total lightning rates increased from 10 flashes min^{-1} to values around 20 flashes min^{-1} by 2010 UTC. This increase in flash rate occurred in conjunction with the development of another strong reflectivity core exceeding 65 dBZ just after 2010 UTC (Figures 9). Large hail (0.75", 0.88") was once again reported between 2010 and 2015 UTC near Damascus, MD. Four of the algorithms (Gatlin, Gatlin 45, 2σ and Threshold 8) activated warnings on the noted increase in lightning around 2010 UTC; however, only the Gatlin algorithms provide any lead time for the report at 2010 UTC because a warning would have already been in effect for this storm (since 1950 UTC). At 2025 UTC 2.00 inch hail was reported in Laytonsville, MD, and at 2030 UTC a funnel cloud was spotted. The timing of reports were in conjunction with a noticeable descent of the latest reflectivity core from around 3 km to just above the surface. The Gatlin, Gatlin 45, 2σ and Threshold 8 algorithms provided nearly 15 minutes of lead time on the large hail. The Threshold 10 and 3σ algorithms still did not recognize a lightning jump because the flash rate and change in flash rate for the storm remained below algorithm triggering limits.

Total lighting increased once again to 25 flashes min^{-1} at 2030 UTC just prior to another increase in vertical growth of the 65 dBZ reflectivity core. The Gatlin, Gatlin 45 and 2σ algorithms were once again activated, as well as the 3σ algorithm, which missed every event prior. The Threshold 10 algorithm had yet to trigger warnings on this storm because DFRDT trends in the total flash rate did not increase beyond 10 flashes min^{-2}. At 2050 UTC, the newest reflectivity core began its descent to the surface. At the same time the total lighting flash rate increased from around 16 flashes min^{-1} to 44 flashes min^{-1}. Between 2050 and 2055 UTC wind damage and hail around 0.75 inches were reported in Central MD, likely in conjunction with the descent of the reflectivity core. The increase in lightning during the

period triggered both the Gatlin algorithms and the Threshold 8 algorithm beginning at 2050 UTC. The lightning activity with the thunderstorm steadily increased as the maximum reflectivity values >65 dBZ disappear (see Figure 9). At 2104 UTC and 2112 UTC 2 additional increases in lightning were observed, and the Gatlin algorithms as well as both Threshold algorithms were triggered once again. The storm decayed as it approached the southern end of Baltimore County. The lightning rate peaked at 49 flashes min^{-1} at 2112 UTC; however, the number of flashes remained steady around 40 flashes min^{-1} through 2126 UTC. The CG flash rate peaked at 8 flashes min^{-1} at 2110 UTC and 2118 and 2122 UTC, and all flashes were of the negative polarity. The core of the storm collapses and large hail and high winds were observed near Baltimore, MD between 2130 and 2145 UTC. The Gatlin and Threshold algorithms provided nearly 30 minutes of warning on this severe weather; however, the 2σ and 3σ algorithms missed the severe weather associated with the demise of the storm.

(iv) 19 June 2007, Null Case

On the morning of June 19, 2007, a mesoscale convective vortex moved across Northern AL (Figure 10). Several convective cells (>35 dBZ) developed well to the east and northeast of the circulation center during the early to mid morning hours (12-14 UTC). These cells contained lightning; however, they remained below severe criteria, and were located far away in East Central TN around the time of a reported tornado. Around 14 UTC the MCV; circulation center entered Northwest AL, with a few convective cells located to the southeast of its center. These cells produced little if any lightning during this time, and the lack of lightning

continued through the time of a tornado that occurred just after 16 UTC. By 1530 UTC additional cells developed just to the east and southeast of the center, and began to rotate relative to the MCV center. At 1605 UTC a small EF0 tornado occurred with no warning in the small community of Trinity, AL, damaging a few homes and garages. WSR-88D radars from KGWX and KHTX were too far away to resolve the circulation; however, the UAH/NSSTC ARMOR radar (Petersen et al. 2005) located closest to the tornadic feature did detect the small circulation. The lack of lightning rendered the use of lightning jump algorithms moot. There is no time height section presented for this thunderstorm because it only reaches the -15°C level for one volume period at 1549 UTC. This case is important though because it illustrates the inability of lightning data to provide warning utility in the event of shallow rotating features which can produce tornadoes.

c. Summary of Algorithm Performance

In this section we present a synthesis of statistical results for the entire dataset of thunderstorms studied. In order to assess the performance of each individual algorithm, POD, FAR, CSI and a HSS values are determined for each algorithm, broken down by range from the individual LMA center.

1) The Gatlin Algorithms

Referring to Table 2 and Table 3, the Gatlin and Gatlin 45 algorithms display a high POD (87% and 97% respectively); however, their FAR is also high, with values of 45% and 55% respectively, when only severe thunderstorms are considered. As mentioned multiple times, the Gatlin algorithm is easily triggered by small changes in the total flash rate. When non-severe thunderstorms are also considered in the sample set, the FARs for these 2 algorithms significantly increase to 65% and 64% . The CSI values just for the severe set are quite strong with values between 51% and 54% ; however, once again when the non-severe thunderstorm dataset is added, the CSI drops by nearly a third to 33% and 36% , respectively. HSS values hover around 0.51 (0.50 for Gatlin and 0.53 for Gatlin 45 at 150 km). Comparing the Gatlin algorithm with 30 minutes of warning length to values presented in Gatlin (2006), the POD is nearly 6% higher than Gatlin's original results while CSI is similar at 55% . Unfortunately, the noted high FAR values eclipse the high POD results, so this algorithm configuration would require considerable improvements prior to being used operationally.

2) The Sigma Algorithms

The statistics for the 2σ algorithm suggest that it shows promise for the detection of severe weather using lightning trend data (Table 4). Examining Table 4, the POD for this algorithm at ranges closer than 100 km is around 87% . The FAR for severe thunderstorms is an impressive 23%. If non-severe thunderstorms are included, the FAR increases to a

modest 33%, which is still much lower than the 48% FAR associated with NWS severe warnings in Barnes et al. (2007). It must be noted though that the sample size in this study is considerably smaller than that presented in Barnes et al. (2007). CSI is slightly higher than the Gatlin algorithms at 69%, and only falls slightly to 61% if the non-severe dataset is included. HSS values are very high with a score of 0.76 for the entire dataset. If the range threshold is expanded 150 km, the above values do not change markedly, indicating that a slight increase in range has little affect on this algorithm. Considering that a perfect HSS value is 1, the above metrics suggest that the 2σ method is a relatively robust algorithm.

The 3σ results are not as promising as the 2σ algorithm. Comparing Table 4 and Table 5, the POD decreases, reaching a value of 50.00% and CSI near 41% within 100 km of the LMA center for the entire dataset. FAR is the lowest of the algorithms at 21% at 100 km or shorter, but this is of little help if the algorithm misses one half of the severe weather events. The decrease in POD and FAR are expected as 3σ algorithm has a slightly higher jump threshold than the 2σ method. Looking once again at Table 5, little if any improvement is found as the domain is extended to 150 km, and the increase in POD may be in part to an increase in the number of severe events. HSS values hover near a respectable 0.58, but the main issue with this algorithm is its POD.

3) The Threshold Algorithms

The threshold based methods also show some promise for severe weather applications. Results presented in Tables 6 and 7 show that these simple threshold-based approaches yield

POD values at 73% for the Threshold 10 method, and 82% for the Threshold 8 method. FARs are manageable for both algorithms, as FARs are 36% and 41% when applied to the entire dataset. As range increases, values of POD, FAR and CSI increase slightly, and this once again may be attributed to the increase in the number of severe events. HSS values are in the mid to upper 0.60 range for both algorithms at either range (Tables 6 and 7), once again indicating promise for severe weather application.

4) Lead Times

Average lead time results for each lightning jump algorithm are very promising. The algorithm that had the largest average lead time was the Gatlin 45 algorithm at 29 minutes. Next, the 2σ algorithm came in with 23 minutes of lead time on average, followed by the Threshold 8 (20 minutes), the Gatlin (19 minutes), the Threshold 10 (15 minutes) and finally the 3σ (12 minutes). No attempt was made to partition lead times for each type of severe weather, as the lightning jump algorithm's purpose is to detect all types of severe weather.

4. Discussion

The use of total lightning data, especially through the filter of a lightning jump algorithm, may provide an expedient means to help forecasters understand what is physically happening in select thunderstorms (e.g, updraft strength and trends in updraft). Traditional

methods for observing thunderstorms (e.g., radar, satellite) will certainly continue to be the "norm"; however, the incorporation of total lightning information and a lightning jump algorithm can be valuable information for warning decisions.

The lightning jump algorithms presented in this study demonstrated skill in their warning application on a variety of thunderstorm types. The 2σ jump algorithm performed best (POD=87%, FAR=33%, HSS=0.75), and exceeded current NWS warning statistics. The FAR value of the 2σ algorithm was nearly 15% below that of the NWS national average presented in Barnes et al. (2007). Additionally, POD for the 2σ algorithm is right in line with the NWS average of 80-90% (T. Troutman, WCM WFO Huntsville, personal communication, 2008). The Threshold 8 algorithm also performed reasonably well despite its relatively simple configuration. The POD value was at the lower end of an acceptable POD for the NWS, however, the Threshold 8 algorithm's FAR value was nearly 7% lower than the average FAR value presented in Barnes et al. (2007). Once again note that there is a considerable difference in each studies' sample size; therefore, these particular algorithms still need further evaluation, especially in meteorological regimes other than Northern AL and Washington D.C.; however, the testing described herein indicates promise of an effective lightning jump algorithm for operational purposes.

Although the Gatlin 45 algorithm provided the largest lead time prior to the occurrence of severe weather at nearly 29 minutes, its high FAR outshines its stellar lead time. If one could sacrifice 6 minutes of lead time, the 2σ algorithm still provides 23 minutes of lead time on average, with a much lower FAR. The Threshold 8 algorithm still provided nearly 20 minutes of lead time on average for severe weather occurrence, which is not too bad considering the average lead time currently for the NWS is about 13 minutes. Again, our

sample size is not as large as the NWS's; however, an average lead time of ten's of minutes in the first stages of lightning jump algorithm development indicate that there will be utility in an operational lightning jump algorithm.

Thunderstorm size clearly played a role in the amount of lightning produced. This was evident during the early stages of the 4 July 2007 thunderstorm near Washington D.C. For comparisons, a 2.00" hail producing supercell thunderstorm from April 8, 2006 used in our dataset will be used. Using the TITAN software, a simple size comparison can be made between the 2 storms (not shown). The April 8th storm was four to seven times larger in size than the July 4th storm just prior to the occurrence of 2.00" hail in each storm. As expected the total flash rates for each storm were dramatically different. The peak 1 minute flash rate for the July 4th storm going back 30 minutes prior to the occurrence of 2.00" hail was 25 flashes per minute. Meanwhile, the peak 1 minute flash rate for the April 8th supercell within 30 minutes prior to the onset of 2.00" hail was 104 flashes per minute. Thus, the size of a given thunderstorm is a significant determinant in the amount of lightning produced, and is a limiting factor for the application of any real-time lightning jump algorithm (especially for a flash rate threshold algorithm) for the detection of severe weather in storms such as the early stages of the July 4, 2007 case.

The representation of storm types in the study was broad, but the number of cases within the thunderstorm dataset needs to be increased. Increasing the sample dataset will allow for a more robust understanding of different thunderstorm types and their associated lightning characteristics, and enable a better determination of the most effective lightning jump threshold value for any of the above configurations. For example, with tropical remnant thunderstorms lightning production is limited; therefore, lower thresholds may be neces-

sary to identify a severe storm in a tropical environment. Finally, statistical modeling is currently being developed to determine the point at which the number of cases studied are reasonable enough to represent a global population of thunderstorms (e.g.,Carey et al. 2009).

5. Conclusions

As a preliminary to GOES-R Geostationary Lightning Mapper algorithm development, this study has developed and tested 6 lightning jump algorithm configurations for operational application. To set the framework for determining the definition or the identification of a severe storm using lightning trends, 69 non-severe thunderstorms were studied to determine what normally occurs within ordinary convection. An average 1 minute peak flash rate from the sample was found to be just above 10 flashes min^{-1}, similar to what past studies have found in Florida (Livingston and Krider 1978). An average DFRDT rate for this same dataset is near 4.74 flashes min^{-2}. Although this number is not used in any of the proposed algorithms, this may be a useful number in the future if a lower bound greater than zero needs to be applied to define the end of a jump. DFRDT rates at the 90 and 93% level of the non-severe sampling distribution were found to be at 8 flashes min^{-2} and 10 flashes min^{-2}, respectively. The average peak flash rate information from this set of storms was used to define a lower limit for triggering the 2σ, 3σ, Threshold 8 and Threshold 10 algorithms. The non-severe peak DFRDT rate information acts as a second level of security for the alarm to sound for the Threshold 8 and Threshold 10 algorithms.

Of the 69 non-severe thunderstorms, all 47 North Alabama cases were tested against each

algorithm to see how many false severe classifications were identified in situations where thunderstorms remained below severe limits. The Gatlin (2006) algorithms performed poorly, with 92 false alarms identified solely in the non-severe database. This is due to the high sensitivity of the algorithm to small increases in total flash rate. The 2σ algorithm performed much better with 16 false alarms triggered, followed by the 3σ with 10, Threshold 8 with 7 and rounding out the bottom the Threshold 10 with 6 false alarms. This information was then incorporated into the statistics after the severe sample is tested.

Severe thunderstorms were broken down by range to see if distance from the center of the LMA had any influence on lightning algorithms. At 100 km, 35 severe thunderstorms with a total of 101 severe weather events were tested against each algorithm. At a range of 150 km, 38 severe thunderstorms were tested with a total of 126 severe weather events. The severe dataset ranges in storm type from isolated supercells to tornadic cells in tropical storm remnants, and all types of severe weather is represented.

A total of 6 algorithm configurations were tested to determine an optimal configuration for a lightning jump algorithm. Of the 6 lightning jump algorithm configurations, the 2σ jump algorithm performed best with POD values at 87%, FAR at 33%, CSI at 61%, and HSS at 0.75. The 2σ jump algorithm's POD was right in line with desired POD values for NWS applications, with a lower FAR by about 15%. Granted, the dataset presented here is much smaller than that presented in Barnes et al. (2007); therefore, more cases from a variety of meteorological regimes are required to examine the full potential of any lightning jump algorithm. The Threshold 8 algorithm may also provide a simple and effective algorithm configuration (POD$\approx$81%, FAR$\approx$41%). The worst performing algorithm was the Gatlin algorithms, primarily due to its high FAR ($\approx$64%). The high FAR value is due to

the algorithm's inclination to trigger on small increases in the total flash rate.

Overall, the use of lightning jump algorithms on many different types of thunderstorms demonstrate that the lightning jump algorithms have the potential to indicate storm severity regardless of environment. Specifically, there is a potential to track severe weather amongst different storm types confined in the GOES-R FOV. However, further testing of the lightning jump algorithms for other areas of the country and meteorological regimes should be conducted to confirm that similar results can be found using any of the lightning jump algorithms presented here, most specifically, the 2σ algorithm.

Acknowledgments.

This work was funded by the GOES-R Risk Reduction effort under Space Act Agreement (NA07AANEG0284). Larry Carey also gratefully acknowledges partial support for this research under an award from the NOAA NWS CSTAR program (NA08NWS4680034). Walt Petersen and Larry Carey acknowledge partial funding of this research via NOAA support of the UAH/NSSTC Tornado and Hurricane Observations Research Center (THOR). The authors would also like to acknowledge John Hall and Jeff Bailey for the NALMA and DCLMA data, as well as, Eugene McCaul and Dennis Buechler for their contributions and help with the LMA datasets and Hugh Christian and William Koshak of NASA MSFC for their continued support and advice throughout this study. A special thanks to Pat Gatlin of ESSC for his technical support with the WDSS-II system. The authors would finally like to thank members of the National Weather Service WFO Huntsville for their insights into

warning operations, specifically WCM Tim Troutman, SOO Chris Darden, and MIC Mike Coyne.

REFERENCES

Barnes, L. R., E. C. Gruntfest, M. H. Hayden, D. M. Schultz, and C. Benight, 2007: False alarms and close calls: a conceptual model of warning accuracy. *Wea. and Forecasting*, **22**, 1140–1147.

Biagi, C. J., K. L. Cummins, K. E. Kehoe, and E. P. Krider, 2007: National Lightning Detection Network (NLDN) performance in southern Arizona, Texas and Oklahoma in 2003-2004. *J. Geophys. Res.*, **112**, doi:10.1029/2006JD007341.

Boccippio, D. J., 2002: Lightning scaling relations revisited. *J. Atmos. Sci.*, **59**, 1086–1104.

Bridenstine, P. V., C. B. Darden, J. Burks, and S. J. Goodman, 2005: The application of total lightning data in the warning decision making process. *Preprints, Conf. on the Meteor. Appl. of Lightning Data*, San Diego, CA, Amer. Meteor. Soc.

Buechler, D. E., K. T. Driscoll, S. J. Goodman, and H. J. Christian, 2000: Lightning activity within a tornadic thunderstorm observed by the Optical Transient Detector (OTD). *Geophys. Res. Lett.*, **27**, 2253–2256.

Byers, H. R. and R. R. Braham, 1949: *The Thunderstorm.* U. S. Government Printing Office, 287 pp.

Carey, L. D., W. A. Petersen, and C. J. Schultz, 2009: A statistical framework for the development and evaluation of a lightning jump algorithm. *Preprints, Fourth Conference on the Meteorological Applications of Lightning Data*, Phoenix, AZ, Amer. Meteor. Soc.

Carey, L. D. and S. A. Rutledge, 1996: A multiparameter radar case study of the microphysical and kinematic evolution of a lightning producing storm. *Meteorol. Atmos. Phys.*, **59**, 33–64.

Carey, L. D. and S. A. Rutledge, 2000: On the relationship between precipitation and lightning in tropical island convection: A C-band polarimetric radar study. *Monthly Weather Review*, **128**, 2687–2710.

Crum, T. D. and R. L. Alberty, 1993: The WSR-88D and the WSR-88D Operational Support Facility. *Bull. Amer. Meteor. Soc.*, **74**, 1669–1687.

Cummins, K. L., J. A. Cramer, C. J. Biagi, E. P. Krider, J. Jerauld, M. A. Uman, and V. A. Rakov, 2006: The US National Lightning Detection Network: Post-upgrade status. *Preprints, 2nd Conf. on Meteorological Applications of Lightning Data*, Atlanta, GA, Amer. Meteor. Soc., CD-ROM, 6.1.

Deierling, W., 2006: *The Relationship Between Total Lightning and Ice Fluxes.* Ph.D, University of Alabama-Huntsville, 175 pp.

Dixon, M. and G. Wiener, 1993: TITAN: Thunderstorm Identification, Tracking Analysis and Nowcasting-A radar-based methodology. *J. Atmos. Ocean Tech.*, **10**, 785–797.

Doswell, C. A., III, R. Davies-Jones, and D. L. Keller, 1990: On summary of skill in rare event forecasting based on contingency tables. *Wea. and Forecasting*, **5**, 576–585.

Gatlin, P., 2006: *Severe Weather Precursors in the Lightning Activity of Tennessee Valley Thunderstorms.* M.S. Thesis, University of Alabama-Huntsville, 87 pp.

Goodman, S. J., R. Blakeslee, H. Christian, W. Koshak, and W. A. Petersen, 2006: GOES-R Lightning Mapper (GLM) research and applications risk reduction. *Preprints, 2nd Symposium Toward a Global Earth Observation System of Systems - Future National Operational Eviron. Satellite Systems*, Atlanta, GA, Amer. Meteor. Soc., CD-ROM P2.2.

Goodman, S. J., D. E. Buechler, P. D. Wright, and W. D. Rust, 1988: Lightning and precipitation history of a microburst-producing storm. *Geophys. Res. Lett.*, **15**, 1185–1188.

Goodman, S. J. and Coauthors, 2005: The North Alabama Lightning Mapping Array: Recent severe storm observations and future prospects. *Atmos. Res.*, **76**, 423–437.

Koshak, W. J. and Coauthors, 2004: North Alabama Lightning Mapping Array (LMA): VHF source retrieval algorithm and error analysis. *J. Atmos. Ocean. Tech.*, **21**, 543–558.

Krehbiel, P. R., 2008: The DC Lightning Mapping Array. *Preprints, 3rd Conf. on Meteorological Applications of Lightning Data*, New Orleans, LA, Amer. Meteor. Soc., 3.2.

Krehbiel, P. R., R. J. Thomas, W. Rison, T. Hamlin, J. Harlin, and M. Davis, 2000: GPS based mapping system retrieval of lightning inside storms. *EOS*, **81**, 21–25.

Lakshmanan, V., T. Smith, K. Hondl, G. J. Stumpf, and A. Witt, 2006: A real-time, three dimensional, rapidly updating, heterogeneous radar merger technique for reflectivity, velocity and derived products. *Wea. and Forecasting*, **21**, 802–823.

Lakshmanan, V., T. Smith, G. J. Stumpf, and K. Hondl, 2007: The warning decision support system - integrated information. *Wea. and Forecasting*, **22**, 596–612.

Lang, T. J. and Coauthors, 2004: The Severe Thunderstorm Electrification and Precipitation Study (STEPS). *Bull. Amer. Meteorol. Soc.*, **85**, 1107–1125.

Livingston, J. M. and E. P. Krider, 1978: Electric fields produced by Florida thunderstorms. *J. Geophys. Res.*, **83**, 385–401.

MacGorman, D. R., D. W. Burgess, V. Mazur, W. D. Rust, W. L. Taylor, and B. C. Johnson, 1989: Lightning rates relative to tornadic storm evolution on 22 May 1981. *J. Atmos. Sci.*, **46**, 221–250.

Motley, S. M., 2006: *Total Lightning Characteristics of Ordinary Convection.* M.S. Thesis, Texas A&M University, 165 pp.

Oye, D. and M. Case, 1995: REORDER: A Program for Gridding Radar Data. Installation and User Manual for the UNIX Version. NCAR Atmospheric Technology Division, Boulder, CO, 19 pp.

Petersen, W. A., H. J. Christian, and S. A. Rutledge, 2005: TRMM observations of the global relationship between ice water content and lightning. *Geophys. Res. Lett.*, **32**, doi: 10.1029/2005GL023236.

Petersen, W. A. and Coauthors, 2005: The UAH-NSSTC/WHNT ARMOR C-band dual-polarimetric radar: A unique collaboration in research, education, and technology transfer. *Preprints of the 32nd AMS Radar Meteorology Conf.*, Albuquerque, NM, Amer. Meteor. Soc.

Proctor, D. E., 1971: A hyperbolic system for obtaining VHF radio pictures of lightning. *J. Geophys. Res.*, **76**, 1478–1489.

Rison, W., R. J. Thomas, P. R. Krehbiel, T. Hamlin, and J. Harlin, 1999: A GPS-based three dimensional lightning mapping system: Initial observations in central New Mexico. *Geophys. Res. Lett.*, **26**, 3573–3576.

Saunders, C. P. R., W. D. Keith, and R. P. Mitzeva, 1991: The effect of liquid water on thunderstorm charging. *J. Geophys. Res.*, **96**, 11 007–11 017.

Steiger, S. M., R. E. Orville, and L. D. Carey, 2007: Total lightning signatures of thunderstorm intensity over North Texas. Part I: Supercells. *Mon. Wea. Rev.*, **135**, 3281–3302.

Steiger, S. M., R. E. Orville, M. J. Murphy, and N. W. S. Demetriades, 2005: Total lightning and radar characteristics of supercells: Insights on electrification and severe weather forecasting. *Preprints, Conf. on the Meteor. Appl. of Lightning Data*, San Diego, CA, Amer. Meteor. Soc., P1.7.

Takahashi, T., 1978: Riming electrification as a charge generation mechanism in thunderstorms. *J. Atmos. Sci.*, **35**, 1536–1548.

Tessendorf, S. A., L. J. Miller, K. C. Wiens, and S. A. Rutledge, 2005: The 29 June 2000 supercell observed during STEPS. Part I: Kinematics and microphysics. *JAS*, **62**, 4127–4150.

Tessendorf, S. A., K. C. Wiens, and S. A. Rutledge, 2007: Radar and lightning observations of the 3 June 2000 electrically inverted storm from STEPS. *Mon. Wea. Rev.*, **135**, 3665–3681.

Thomas, R. P., P. R. Krehbiel, W. Rison, S. Hunyady, W. Winn, T. Hamlin, and

J. Harlin, 2004: Accuracy of the lightning mapping array. *J. Geophys. Res.*, **109**, doi: 10.1029/2004JD004549.

Trapp, R. J., D. M. Wheatly, N. T. Atkins, and R. W. Przybylinkski, 2005: Buyer beware: Some words of caution on the use of severe wind reports in postevent assessment and research. *Wea. and Forecasting*, **21**, 408–415.

Vonnegut, B., 1963: Some facts and speculation concerning the origin and role of thunderstorm electricity. *Severe Local Storms, Meteor. Monogr.*, Amer. Meteor. Soc., 224–241.

Weiss, S. J., J. A. Hart, and P. R. Janish, 2002: An examination of severe thunderstorm wind report climatology: 1970-1999. *Preprints, 21st Conf. on Severe Local Storms*, San Antonio, TX, Amer. Meteor. Soc., 446-449.

Wiens, K. C., S. A. Rutledge, and S. A. Tessendorf, 2005: The 29 June 2000 supercell observed during steps. Part II: Lightning and charge structure. *J. Atmos. Sci.*, **62**, 4151–4177.

Wilks, D. S., 1995: *Statistical Methods in the Atmospheric Sciences.* Academic Press, 467 pp.

Williams, E. R., 1985: Large scale charge separation in thunderclouds. *J. Geophys. Res.*, **90**, 6013–6025.

Williams, E. R., 1989a: The tripole structure of thunderstorms. *J. Geophys. Res.*, **94**, 13 151–13 167.

Williams, E. R. and Coauthors, 1999: The behavior of total lightning activity in severe Florida thunderstorms. *Atmos. Res.*, **51**, 245–265.

Wilson, N. L., D. W. Breed, T. R. Saxen, and N. W. S. Demetriades, 2006: The utility of total lightning in convective nowcasting. *Preprints, 19th Int. Lightning Meteor. Conf.*, Tuscon, AZ, Vaisala Inc.

Witt, A., M. D. Eilts, G. J. Stumpf, E. D. Mitchell, J. T. Johnson, and K. W. Thomas, 1998b: Evaluating the performance of WSR-88D severe storm detection algorithms. *Wea. and Forecasting*, **13**, 513–518.

Workman, E. J. and S. E. Reynolds, 1949: Electrical activity as related to thunderstorm cell growth. *Bull. Amer. Meteor. Soc.*, **30**, 142–144.

List of Tables

1	Number of False Alarms for Non-Severe Convection	43
2	Results for the Gatlin Algorithm with a 30 minute warning length.	44
3	Results for the Gatlin Algorithm with a 45 minute warning length.	45
4	Results for the 2σ algorithm with a 45 minute warning length.	46
5	Results for the 3σ algorithm with a 45 minute warning length.	47
6	Results for the Threshold 10 Algorithm with a 45 minute warning length.	48
7	Results for the Threshold 8 algorithm with a 45 minute warning length.	49

TABLE 1. Number of False Alarms for Non-Severe Convection

	Gatlin	2σ	3σ	Threshold 10	Threshold 8
No. of False Alarms	92	16	10	6	7

TABLE 2. Results for the Gatlin Algorithm with a 30 minute warning length.

	POD	FAR	CSI	HSS
Within 100 km				
Severe only	87%	45%	51%	0.67
Severe and Non-Severe	87%	65%	33%	0.50
Within 150 km				
Severe only	80%	52%	46%	0.63
Severe and Non-Severe	89%	66%	33%	0.50

TABLE 3. Results for the Gatlin Algorithm with a 45 minute warning length.

	POD	FAR	CSI	HSS
Within 100 km				
Severe only	97%	55%	55%	0.71
Severe and Non-Severe	97%	64%	37%	0.53
Within 150 km				
Severe only	98%	49%	51%	0.67
Severe and Non-Severe	98%	63%	36%	0.53

TABLE 4. Results for the 2σ algorithm with a 45 minute warning length.

	POD	FAR	CSI	HSS
Within 100 km				
Severe only	87%	23%	69%	0.82
Severe and Non-severe	87%	33%	61%	0.76
Within 150 km				
Severe only	87%	26%	67%	0.80
Severe and Non-Severe	87%	33%	61%	0.75

TABLE 5. Results for the 3σ algorithm with a 45 minute warning length.

	POD	FAR	CSI	HSS
Within 100 km				
Severe only	50%	20%	44%	0.61
Severe and Non-severe	50%	32%	41%	0.58
Within 150 km				
Severe only	56%	21%	49%	0.65
Severe and Non-Severe	56%	29%	45%	0.62

TABLE 6. Results for the Threshold 10 Algorithm with a 45 minute warning length.

	POD	FAR	CSI	HSS
Within 100 km				
Severe only	73%	32%	54%	0.70
Severe and Non-severe	73%	36%	52%	0.68
Within 150 km				
Severe only	72%	37%	51%	0.67
Severe and Non-Severe	72%	40%	49%	0.66

TABLE 7. Results for the Threshold 8 algorithm with a 45 minute warning length.

	POD	FAR	CSI	HSS
Within 100 km				
Severe only	82%	37%	55%	0.71
Severe and Non-severe	82%	41%	52%	0.69
Within 150 km				
Severe only	83%	42%	52%	0.68
Severe and Non-Severe	83%	42%	50%	0.67

List of Figures

1 Presented here is the histogram of 69 non-severe thunderstorm peak flash rates (flashes min^{-1}). The average peak flash rate for the entire dataset of non-severe thunderstorms was 10 flashes min^{-1}. 54

2 Presented here is the histogram of 69 non-severe thunderstorm peak DFRDT rates (flashes min^{-2}). The 90% level is near 8 flashes min^{-2} and the 93% level is near 10 flashes min^{-2}. 55

3 This is an example of the visual TITAN output taken from April 4, 2007, at 0306 UTC from KHTX. Shaded areas represent where dBZ values are greater than 35 dBZ at a height of -15°C. For this case that level is located at 6 km and each shaded region was used to locate and track individual intense thunderstorm cells. Each intense thunderstorm is easily identifiable despite the complex structure of this MCS. 56

4 Presented in this figure are four constant altitude plan position indicator (CAPPI) plots of reflectivity from KHTX between 0257 and 0331 UTC on April 4, 2007 at 2 km altitude. An MCS approached Northern Alabama from the northwest, and there were several areas of interest along the line. At 0257 UTC (upper left) there were 2 distinct cells out ahead of the line. The cell enclosed by a black rectangle was the thunderstorm that merged with the line and contributed to the further development of severe weather. The black rectangle follows the progression of the thunderstorm throughout the image. At 0306 UTC (upper right) the cell has now merged with the main line and enhanced the reflectivity along the southwestern end of the line. The cell that was just ahead of the line is still somewhat isolated. By 0314 UTC (lower left) both cells have been enveloped by the MCS. At 0331 UTC evidence of a small notch is present in Northern Madison County, AL, which is about the time the tornado was still on the ground. 57

5 Presented here is the time-height plot from Thunderstorm A using reflectivity data from KHTX on April 4, 2007. Reflectivity contours are every 5 dB, total flash rate (flashes min^{-1}) is represented by the solid purple line, and the solid blue line represents VIL (kg m^{-3}). The merge with the MCS occurred between 0300 and 0310 UTC, and was identified by the increase in the total flash rate and in 35 dBZ echo top height. The analysis period ends when the individual cell that is being tracked falls below the -15°C height. 58

6 Presented here is a reflectivity CAPPI from KBMX at 1954 UTC on September 25, 2005 at 2 km altitude. Reflectivity units are in dBZ, and are contoured every 10 dB. The tornadic cell (inset) is located in Central Winston Co. AL, near the town of Double Springs, about 90 km to the northwest of Birmingham, AL. 2 tornado touchdowns were reported at 1954 and 1957 UTC nearly 30 minutes after an increase in lightning triggered the Gatlin and Sigma Algorithms. 59

7 Represented here is the time-height plot from Thunderstorm A using reflectivity data from KBMX on September 25, 2005. Total flash rate (flashes min^{-1}) is represented by the solid purple line, and the solid blue line represents VIL (kg m^{-3}). A strong reflectivity core developed just before there is an increase in the total flash rate between 1923 and 1927 UTC. Around this same time 35 dBZ echo tops increased from 8 to 9 km. 60

8 Presented here is a reflectivity CAPPI from KLWX on July 4, 2007, at 2025 UTC. Reflectivity units are in dBZ, and are contoured every 10 dB. Several isolated thunderstorms developed during the afternoon hours across Northern VA and MD. The thunderstorm of interest is in Howard Co., MD at this time, which is about 40 km to the north of Washington D.C. (inset) 61

9 Presented here is the time-height plot from Thunderstorm A using reflectivity from KLWX on July 4, 2007. Reflectivity contours are every 5 dB, total flash rate (flashes min^{-1}) is represented by the solid purple line, and the solid blue line represents VIL (kg m^{-3}). This thunderstorm actually existed below the minimal detection threshold for TITAN for one hour, and then around 1934 UTC underwent substantial vertical growth. Very strong reflectivity values were found ($>$ 65 dBZ). For the first stages of the thunderstorm, the flash rate only peaked near 25 flashes min^{-1}, but by 2100 UTC increased to just over 40 flashes min^{-1}. 62

10 Presented here is a reflectivity CAPPI from KHTX on June 19, 2007 at 1554 UTC at an altitude of 2 km. Reflectivity units are in dBZ, and are contoured every 10 dB. This is just prior to the tornado formation near Trinity, AL, about 100 km to the southwest of KHTX. The area of interest is located just to the northeast of the MCV circulation (inset). The NWS WSR-88D radars were located too far away to sample the small circulation, however, the UAH/NSSTC ARMOR radar was able to observe the circulation as it passed through the town of Trinity. 63

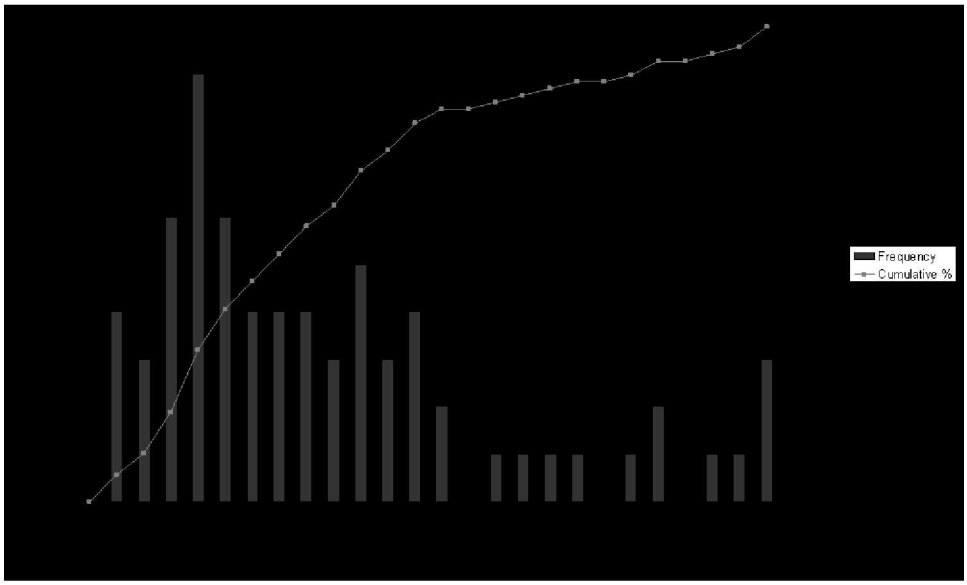

FIG. 1. Presented here is the histogram of 69 non-severe thunderstorm peak flash rates (flashes min^{-1}). The average peak flash rate for the entire dataset of non-severe thunderstorms was 10 flashes min^{-1}.

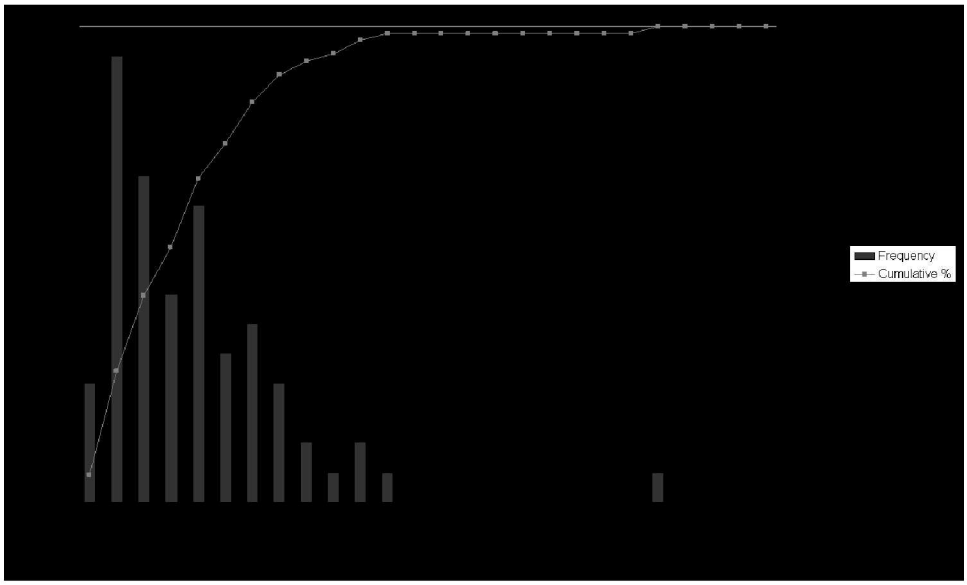

FIG. 2. Presented here is the histogram of 69 non-severe thunderstorm peak DFRDT rates (flashes min^{-2}). The 90% level is near 8 flashes min^{-2} and the 93% level is near 10 flashes min^{-2}.

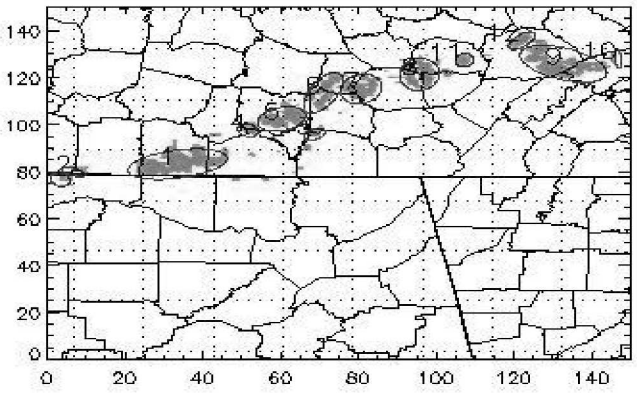

FIG. 3. This is an example of the visual TITAN output taken from April 4, 2007, at 0306 UTC from KHTX. Shaded areas represent where dBZ values are greater than 35 dBZ at a height of -15°C. For this case that level is located at 6 km and each shaded region was used to locate and track individual intense thunderstorm cells. Each intense thunderstorm is easily identifiable despite the complex structure of this MCS.

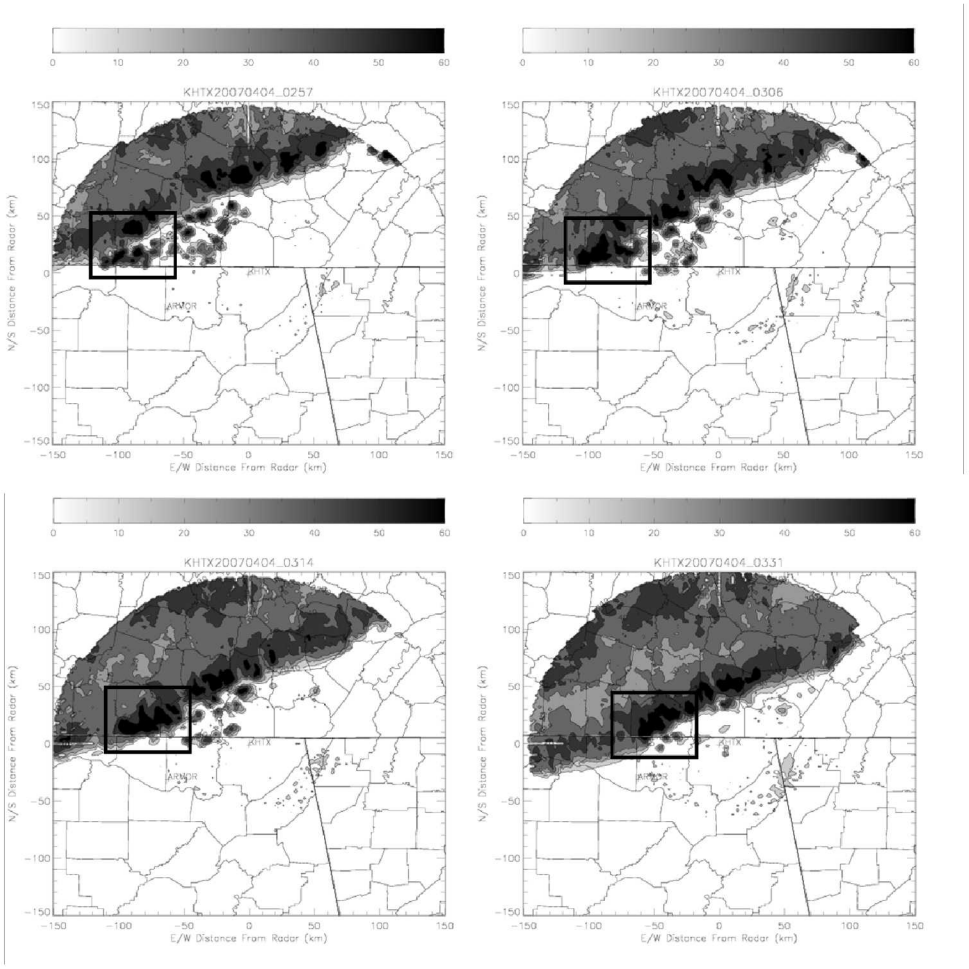

FIG. 4. Presented in this figure are four constant altitude plan position indicator (CAPPI) plots of reflectivity from KHTX between 0257 and 0331 UTC on April 4, 2007 at 2 km altitude. An MCS approached Northern Alabama from the northwest, and there were several areas of interest along the line. At 0257 UTC (upper left) there were 2 distinct cells out ahead of the line. The cell enclosed by a black rectangle was the thunderstorm that merged with the line and contributed to the further development of severe weather. The black rectangle follows the progression of the thunderstorm throughout the image. At 0306 UTC (upper right) the cell has now merged with the main line and enhanced the reflectivity along the southwestern end of the line. The cell that was just ahead of the line is still somewhat isolated. By 0314 UTC (lower left) both cells have been enveloped by the MCS. At 0331 UTC evidence of a small notch is present in Northern Madison County, AL, which is about the time the tornado was still on the ground.

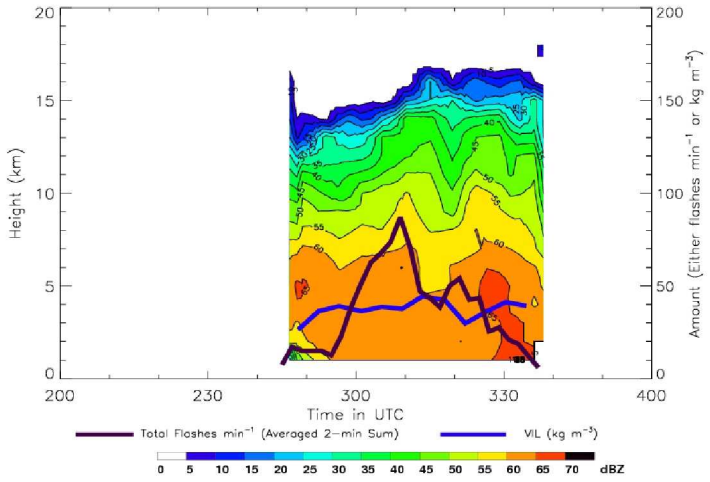

FIG. 5. Presented here is the time-height plot from Thunderstorm A using reflectivity data from KHTX on April 4, 2007. Reflectivity contours are every 5 dB, total flash rate (flashes min^{-1}) is represented by the solid purple line, and the solid blue line represents VIL (kg m^{-3}). The merge with the MCS occurred between 0300 and 0310 UTC, and was identified by the increase in the total flash rate and in 35 dBZ echo top height. The analysis period ends when the individual cell that is being tracked falls below the -15°C height.

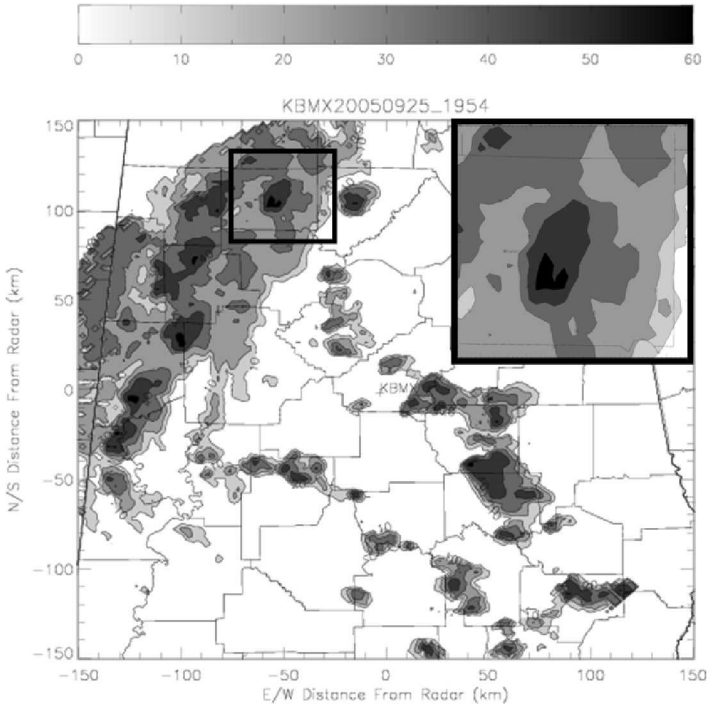

FIG. 6. Presented here is a reflectivity CAPPI from KBMX at 1954 UTC on September 25, 2005 at 2 km altitude. Reflectivity units are in dBZ, and are contoured every 10 dB. The tornadic cell (inset) is located in Central Winston Co. AL, near the town of Double Springs, about 90 km to the northwest of Birmingham, AL. 2 tornado touchdowns were reported at 1954 and 1957 UTC nearly 30 minutes after an increase in lightning triggered the Gatlin and Sigma Algorithms.

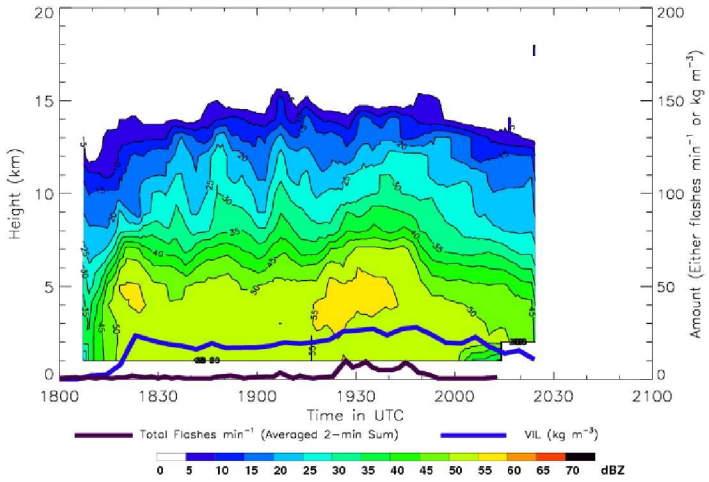

FIG. 7. Represented here is the time-height plot from Thunderstorm A using reflectivity data from KBMX on September 25, 2005. Total flash rate (flashes min^{-1}) is represented by the solid purple line, and the solid blue line represents VIL (kg m^{-3}). A strong reflectivity core developed just before there is an increase in the total flash rate between 1923 and 1927 UTC. Around this same time 35 dBZ echo tops increased from 8 to 9 km.

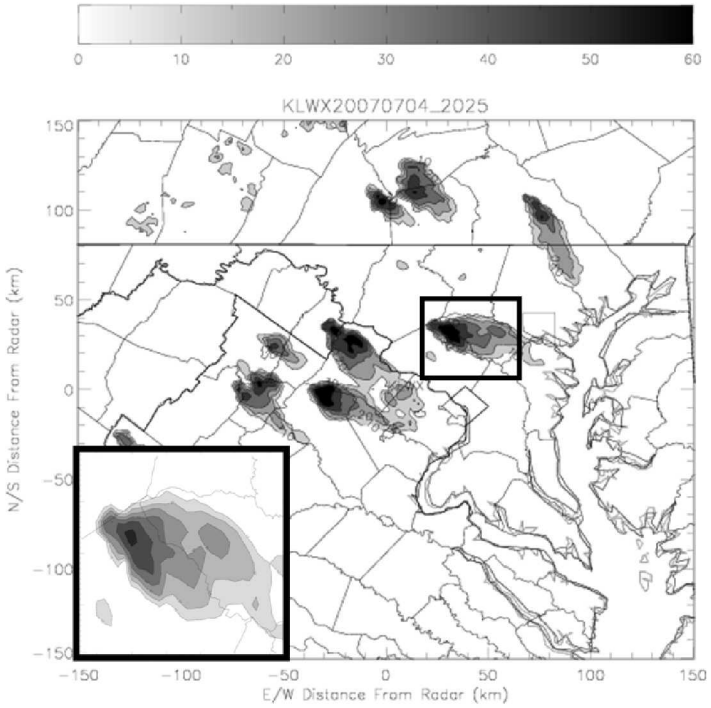

FIG. 8. Presented here is a reflectivity CAPPI from KLWX on July 4, 2007, at 2025 UTC. Reflectivity units are in dBZ, and are contoured every 10 dB. Several isolated thunderstorms developed during the afternoon hours across Northern VA and MD. The thunderstorm of interest is in Howard Co., MD at this time, which is about 40 km to the north of Washington D.C. (inset)

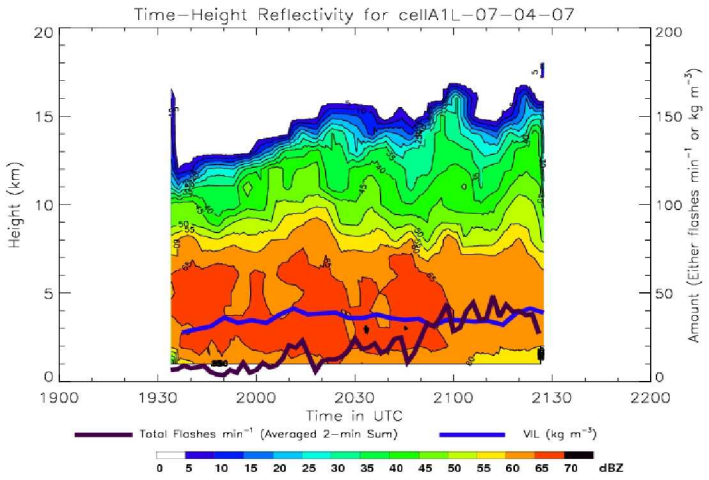

FIG. 9. Presented here is the time-height plot from Thunderstorm A using reflectivity from KLWX on July 4, 2007. Reflectivity contours are every 5 dB, total flash rate (flashes min^{-1}) is represented by the solid purple line, and the solid blue line represents VIL (kg m^{-3}). This thunderstorm actually existed below the minimal detection threshold for TITAN for one hour, and then around 1934 UTC underwent substantial vertical growth. Very strong reflectivity values were found (> 65 dBZ). For the first stages of the thunderstorm, the flash rate only peaked near 25 flashes min^{-1}, but by 2100 UTC increased to just over 40 flashes min^{-1}.

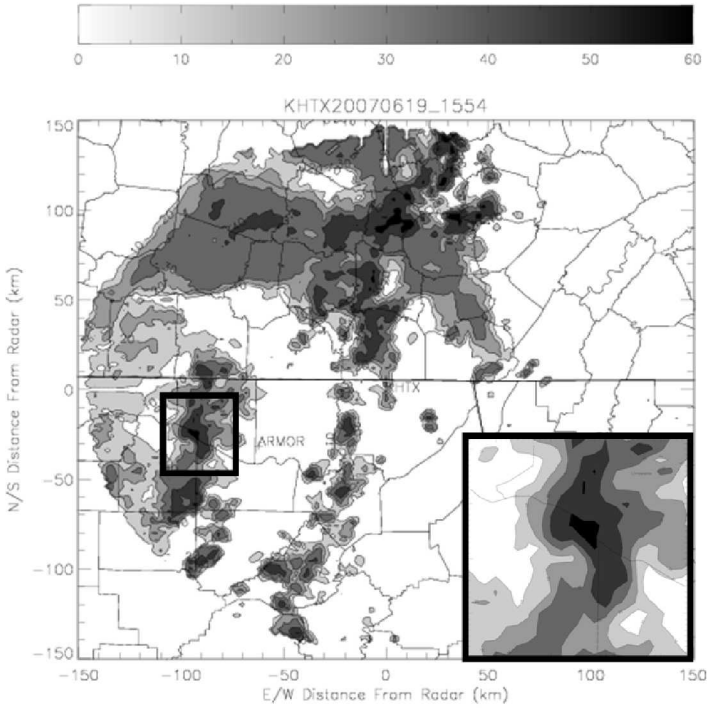

FIG. 10. Presented here is a reflectivity CAPPI from KHTX on June 19, 2007 at 1554 UTC at an altitude of 2 km. Reflectivity units are in dBZ, and are contoured every 10 dB. This is just prior to the tornado formation near Trinity, AL, about 100 km to the southwest of KHTX. The area of interest is located just to the northeast of the MCV circulation (inset). The NWS WSR-88D radars were located too far away to sample the small circulation, however, the UAH/NSSTC ARMOR radar was able to observe the circulation as it passed through the town of Trinity.